Atmos. Chem. Phys., 13, 8439–8455, 2013
www.atmos-chem-phys.net/13/8439/2013/
doi:10.5194/acp-13-8439-2013

Atmospheric Chemistry and Physics Open Access

Understanding the impact of recent advances in isoprene photooxidation on simulations of regional air quality

Y. Xie[1], F. Paulot[2,*], W. P. L. Carter[3], C. G. Nolte[1], D. J. Luecken[1], W. T. Hutzell[1], P. O. Wennberg[2], R. C. Cohen[4], and R. W. Pinder[1]

[1]US EPA Office of Research and Development, Durham, North Carolina, USA
[2]California Institute of Technology, Pasadena, California, USA
[3]University of California, Riverside, Riverside, California, USA
[4]University of California, Berkeley, Berkeley, California, USA
[*]now at: Harvard University, Cambridge, Massachusetts, USA

Correspondence to: R. W. Pinder (pinder.rob@epa.gov)

Received: 5 September 2012 – Published in Atmos. Chem. Phys. Discuss.: 17 October 2012
Revised: 26 January 2013 – Accepted: 12 July 2013 – Published: 27 August 2013

Abstract. The CMAQ (Community Multiscale Air Quality) us model in combination with observations for INTEX-NA/ICARTT (Intercontinental Chemical Transport Experiment–North America/International Consortium for Atmospheric Research on Transport and Transformation) 2004 are used to evaluate recent advances in isoprene oxidation chemistry and provide constraints on isoprene nitrate yields, isoprene nitrate lifetimes, and NO_x recycling rates. We incorporate recent advances in isoprene oxidation chemistry into the SAPRC-07 chemical mechanism within the US EPA (United States Environmental Protection Agency) CMAQ model. The results show improved model performance for a range of species compared against aircraft observations from the INTEX-NA/ICARTT 2004 field campaign. We further investigate the key processes in isoprene nitrate chemistry and evaluate the impact of uncertainties in the isoprene nitrate yield, NO_x ($NO_x = NO + NO_2$) recycling efficiency, dry deposition velocity, and $RO_2 + HO_2$ reaction rates. We focus our examination on the southeastern United States, which is impacted by both abundant isoprene emissions and high levels of anthropogenic pollutants. We find that NO_x concentrations increase by 4–9 % as a result of reduced removal by isoprene nitrate chemistry. O_3 increases by 2 ppbv as a result of changes in NO_x. OH concentrations increase by 30 %, which can be primarily attributed to greater HO_x production. We find that the model can capture observed total alkyl and multifunctional nitrates ($\sum$ANs) and their relationship with O_3 by assuming either an isoprene nitrate yield of 6 % and daytime lifetime of 6 hours or a yield of 12 % and lifetime of 4 h. Uncertainties in the isoprene nitrates can impact ozone production by 10 % and OH concentrations by 6 %. The uncertainties in NO_x recycling efficiency appear to have larger effects than uncertainties in isoprene nitrate yield and dry deposition velocity. Further progress depends on improved understanding of isoprene oxidation pathways, the rate of NO_x recycling from isoprene nitrates, and the fate of the secondary, tertiary, and further oxidation products of isoprene.

1 Introduction

Isoprene emissions are the dominant source of non-methane volatile organic compounds to the atmosphere (Guenther et al., 2006). Being highly reactive (lifetime ~ 3 h at OH concentration of 1×10^6 mol cm^{-3}), isoprene plays a central role in tropospheric chemistry. When isoprene reacts with OH, six isomeric hydroperoxy radicals ($ISOPO_2$) are formed. When NO concentrations are greater than ~ 150 ppt, $ISOPO_2$ primarily reacts with NO to yield mainly alkoxy radicals and NO_2. Subsequently, O_3 is formed through NO_2 photolysis, while OH and NO are regenerated in autocatalytic cycles. The minor channel forms hydroxynitrates (ISOPN, Table 1), which sequester NO_x and therefore regulate O_3 formation locally. There have been a number of laboratory studies reporting the ISOPN yield, with the value

ranging from 4.4 % to 15 % (Tuazon and Atkinson, 1990; Chen et al., 1998; Chuong and Stevens, 2002; Sprengnether et al., 2002; Patchen et al., 2007; Paulot et al., 2009a; Lockwood et al., 2010).

With the presence of a double bond, ISOPNs are highly reactive with respect to OH and O_3 (Giacopelli et al., 2005; Paulot et al., 2009a; Lockwood et al., 2010). At OH concentration of 1×10^6 mol cm^{-3} and 40 ppbv O_3, the lifetime of ISOPN with respect to OH is about 4 h (Paulot et al., 2009a) and to O_3 is about 3 h (Lockwood et al., 2010), giving a combined lifetime slightly less than 2 h. The products from ISOPN oxidation might either retain the nitrate functionality (Grossenbacher et al., 2001; Giacopelli et al., 2005; Perring et al., 2009a) or release NO_x (Paulson and Seinfeld, 1992). Paulot et al. (2009a) estimate about 50 % recycling efficiency of NO_x (α) from ISOPN + OH/NO reactions and identified some of the organic nitrates produced by this reaction, including methyl vinyl ketone nitrate, methacrolein nitrate, and propanone nitrate. A recent field study confirmed the existence of these secondary organic nitrates compounds (Beaver et al., 2012). Some of these organic nitrates products, e.g., propanone nitrate, are found to be considerably longer-lived than ISOPN and can serve as temporary reservoirs for NO_x, thereby impacting the NO_y budget as well as O_3 levels far from isoprene source region (Paulot et al., 2009a; 2012). The products and NO_x recycling efficiency from ISOPN oxidation by O_3 are poorly understood (Giacopelli et al., 2005; Lockwood et al., 2010).

Furthermore, there are also large uncertainties in isoprene+NO_3 oxidation chemistry. Although only accounting for about 6–7 % of isoprene oxidation (Horowitz et al., 2007; Ng et al., 2008), studies suggest that isoprene can be an important sink for NO_3 radical (Starn et al., 1998; Brown et al., 2009), and the reaction contributes substantially (30–60 %) to the formation of isoprene nitrates (ING) (von Kuhlmann et al., 2004; Horowitz et al., 2007; Paulot et al., 2012). The isoprene+NO_3 reaction is initiated by NO_3 addition to a double bond, followed by reaction with O_2 to produce a nitroxy peroxy radical ($NISOPO_2$). Subsequent reaction of $NISOPO_2$ with NO, NO_3, RO_2, and HO_2 can either result in functionalization, conserving the nitrate group, or release NO_2 through dissociation. Large nitrates yields ($\sim$ 80 %) have been reported in a number of experimental studies (Barnes et al., 1990; Berndt and Boge, 1997; Rollins et al., 2009; Perring et al., 2009b; Kwan et al., 2012), with the primary products identified as C5-nitrooxycarbonyl (NIT1), C5-nitrooxyhydroperoxide (NISOPOOH), and C5-hydroxynitrate (ISOPN). Few studies have investigated the fate of these organic nitrates (Rollins et al., 2009); therefore, their oxidation products and NO_x recycling efficiency are not well known.

In addition to photochemical loss, isoprene nitrates are also subject to removal by deposition. Measurements have found these multi-functional nitrates are soluble in water with large Henry's law constants (Shepson et al., 1996; Treves et al., 2000). Their dry deposition velocities are less constrained, with measured values ranging from that of PAN (0.4 cm s^{-1}, Shepson et al., 1996) to HNO_3 (2.7 cm s^{-1}, Farmer and Cohen, 2008). Studies also disagree regarding the relative importance of removal by deposition (Horowitz et al., 2007) and removal by photooxidation (Shepson et al., 1996; Ito et al., 2007; Perring et al., 2009a).

Simulations of tropospheric ozone production are known to be highly sensitive to ISOPN yield (von Kuhlmann et al., 2004; Wu et al., 2007; Ito et al., 2007; Weaver et al., 2009; Paulot et al., 2012). For example, Wu et al. (2007) found a 10 % reduction in global tropospheric ozone production while increasing the ISOPN yield from 4 % to 12 %. Similar to the effects of ISOPN yield, recent work by Paulot et al. (2012) also highlighted the importance of NO_x recycling efficiency as well as the representation of secondary nitrate photochemistry for the simulation of tropical ozone.

In additional to laboratory studies, field observations have been used to probe isoprene nitrate chemistry. For example, Horowitz et al. (2007) found that a 40 % recycling efficiency together with a 4 % ISOPN yield and a fast dry deposition rate best captured the alkyl and multifunctional nitrates measurements collected during the INTEX-NA/ICARTT (Intercontinental Chemical Transport Experiment–North America/International Consortium for Atmospheric Research on Transport and Transformation) field study during summer 2004 (Singh et al., 2006; Fehsenfeld et al., 2006). Using the same datasets, Perring et al. (2009a) inferred a NO_x recycling efficiency between 3 % and 33 % depending on the assumed ISOPN yields (4 – 12 %).

Recently, there have also been many studies devoted to isoprene oxidation under low NO_x conditions (Lelieveld et al., 2008; Paulot et al., 2009b; Peeters et al., 2009; Peeters and Müller, 2010; Crounse et al., 2011). These studies address some of the important challenges with isoprene chemistry including (i) the apparent discrepancy between observed and modeled HO_x abundance under isoprene rich conditions (Thornton et al., 2002; Ren et al., 2008; Butler et al., 2008; Lelieveld et al., 2008); and (ii) the link between isoprene gas phase oxidation and the formation of organic aerosols (Claeys et al., 2004; Edney et al., 2005; Kleindienst et al., 2007; Paulot et al., 2009b; Surratt et al., 2010).

The tropical forest has been a focus area for many recent studies (Lelieveld et al., 2008; Butler et al., 2008; Karl et al., 2009; Stone et al., 2011; Whalley et al., 2011) that aim to improve the understanding of isoprene oxidation chemistry. These locations are mostly characterized by very large biogenic emissions with pristine conditions, where isoprene peroxy radicals are dominated by reactions with HO_2 and isomerization. Nevertheless, anthropogenic emissions are known to substantially affect the relative importance of isoprene oxidation pathways and products (e.g., alkyl and multifunctional nitrates, epoxides). The southeastern United States is a region known for its abundant isoprene emissions and anthropogenic pollutants, providing a good opportunity

Table 1. Speciated alkyl and multifunctional nitrates in the IS scheme.

Group		Species	Description
isoprene nitrates (ING)	ING_0	ISOPND	$\delta-$hydroxy isoprene nitrate
		ISOPNB	$\beta-$hydroxy isoprene nitrate
		NIT1	C5-nitrooxycarbonyl
		NISOPOOH	C5-nitrooxyhydroperoxide
	ING_1	MVKN	methylvinylketone nitrate
		MACRN	methacrolein nitrate
		ETHLN	ethanal nitrate
		RNO3I	lumped organic nitrates from isoprene
	ING_2	PROPNN	propanone nitrate formed from isoprene + OH
		PROPNNB	propanone nitrate formed from isoprene + NO_3
other alkyl and multifunctional nitrates		RNO3	lumped organic nitrates from sources other than isoprene

to understand the impact of isoprene nitrates in a region influenced by both biogenic emissions and a range of NO_x concentrations.

In this study, we incorporate recent advances in isoprene oxidation chemistry into the SAPRC-07 chemical mechanism (Carter, 2010a) within the US EPA Community Multiscale Air Quality (CMAQ) model (Byun and Schere, 2006). Data from the INTEX-NA/ICARTT campaign during the summer of 2004 (Singh et al., 2006; Fehsenfeld et al., 2006) are used to evaluate model performance and constrain the uncertainties in the isoprene nitrate chemistry. The observations include measurements of speciated NO_y, organic compounds, and aerosols, comprising a comprehensive dataset for characterizing the summer continental boundary layer of the eastern United States. In contrast to previous modeling studies, we use a highly detailed representation of isoprene chemistry and examine the effect on areas where both biogenic and anthropogenic emissions are important. In Sect. 2, we describe the modeling system and the updated isoprene oxidation scheme. In Sect. 3.1, we evaluate the CMAQ model results with INTEX-NA/ICARTT observations. We further investigate the sources and sinks of the isoprene peroxy radicals and isoprene nitrates (Sects. 3.2 and 3.3). We then examine the sensitivity of model results to the most important uncertainties in our current understanding of isoprene nitrate chemistry (Sect. 3.4), with an emphasis on O_3 and OH concentrations (Sect. 3.5).

2 Methods and data

We start this section by describing the updates to isoprene oxidation chemistry, followed by discussion of the photochemical modeling system and the observational datasets used to constrain the model results.

2.1 Updated isoprene oxidation scheme

We base our core chemistry on a modified version of SAPRC-07, including changes for air toxics (i.e., SAPRC-07T (Hutzell et al., 2012), referred to as the BASE scheme). A new version of the mechanism is developed in this study (referred to as the standard isoprene scheme (IS)), which incorporates recent advances in isoprene oxidation chemistry (Paulot et al., 2009a, b; Lockwood et al., 2010; Peeters and Müller, 2010; Crounse et al., 2011; Rollins et al., 2009). The changes include a more explicit representation of isoprene nitrate formation from OH/NO and NO_3 pathways as well as modification to the isoprene chemistry under low-NO_x conditions. The updated chemistry is summarized in Fig. 1; see Tables S1 and S2 (Supplement) for a complete listing of the compounds and reactions. Each of the speciated isoprene nitrates is described in Table 1.

In the standard SAPRC-07 mechanism (Carter, 2010a, b), isoprene nitrates are represented, along with all other non-PAN analogue organic nitrates, as a lumped organic nitrate species (RNO_3), with k_{OH} of 7.2×10^{-12} cm^3 mol^{-1} s^{-1} and NO_x recycling efficiency of about 30 %. In the OH/NO reactions of isoprene, the RNO_3 yield is 9.3 %. This RNO_3 yield is a derived value. It is treated as a parameter and adjusted to improve the comparison of SAPRC-07 simulated O_3 measurements from laboratory chamber experiments. The O_3 comparison is very sensitive to the RNO_3 yield parameter. In the NO_3 oxidation pathway, a large fraction (75 %) of organic nitrates is assumed to be long-lived and is treated as lost nitrogen (XN), and the RNO_3 yield is only 6.4 %.

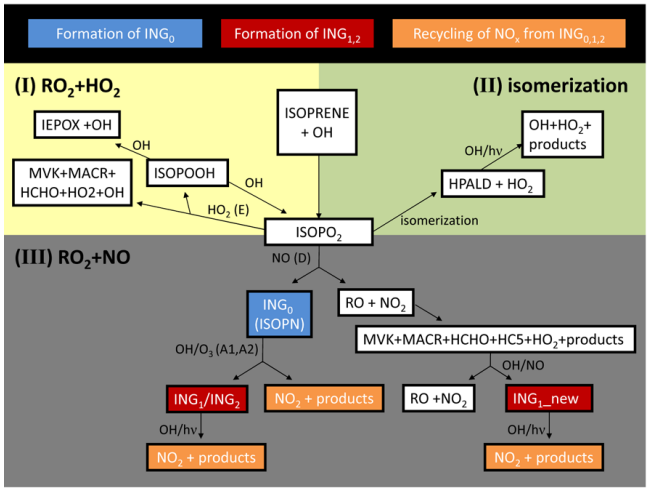

Fig. 1a. Updated oxidation scheme for isoprene + OH, noting the formation of first generation isoprene nitrates (ING_0), later generation isoprene nitrates ($ING_{1,2}$), and recycling of NO_x from isoprene nitrates. Reactions modified by the sensitivity studies in Sect. 3.4 are denoted by the letters in parentheses (A–E).

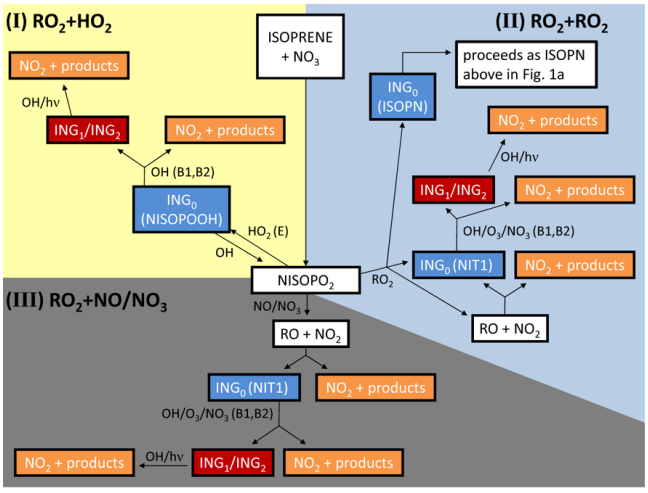

Fig. 1b. Updated oxidation scheme for isoprene + NO_3. The colors retain the same meaning as in Fig. 1a.

The IS mechanism treats isoprene nitrates explicitly. Isoprene oxidation reactions from OH are shown in Fig. 1a. In the presence of NO, isoprene nitrates can form as described by Pathway III in Fig. 1a. The formation and the subsequent oxidation of organic nitrates are largely based on the work of Paulot et al. (2009a). The δ- and β-hydroxy isoprene nitrates (ISOPN) are represented separately, as their fate varies substantially from each other (Paulot et al., 2009a). Formation and photooxidation of organic nitrates from MVK and MACR, i.e., methyl vinyl ketone nitrate (MVKN) and methacrolein nitrate (MACRN), are also treated following Paulot et al. (2009a). ISOPN reacts rapidly with OH (weighted average $k_{OH} = 6.2 \times 10^{-11}$ cm^3 mol^{-1} s^{-1} for δ- and β-branch), releasing about 60 % of NO_x, with the rest forming methyl vinyl ketone nitrate (MVKN), methacrolein nitrate (MACRN), propanone nitrate (PROPNN), and ethanal nitrate (ETHLN). PROPNN reaction with OH (Zhu et al., 1991; Paulot et al., 2012) and photolysis (Roberts and Fajer, 1989; Barnes et al., 1993; Saunders et al., 2003) are added, and PROPNN is substantially longer-lived ($k_{OH} = 4.0 \times 10^{-13}$ cm^3 mol^{-1} s^{-1}) than other second-generation isoprene nitrates. Photolysis rates of MVKN and ETHLN are assumed to be the same as that of PROPNN. For ISOPN+O_3 reactions, we use the reaction rate coefficients (weighted average $k_{O_3} = 8.4 \times 10^{-17}$ cm^3 mol^{-1} s^{-1}) from Lockwood et al. (2010). As little is known about the products and NO_x recycling efficiency from this pathway, we estimate the likely products largely based on the SAPRC mechanism generation system (Carter, 2000, 2010b). We assume a lower NO_x recycling (30 %) from ISOPN + O_3 than from ISOPN+OH/NO reactions. In addition to the species listed above, a general isoprene nitrate species (RNO_3I) is added to represent additional second-generation organic nitrates formation. RNO_3I is assumed to react readily with OH ($k_{OH} = 8 \times 10^{-12}$ cm^3 mol^{-1} s^{-1}).

The oxidation of isoprene by NO_3 (Fig. 1b) is also updated in the IS mechanism. A nitrooxy-carbonyl (NIT1) yield of 70 % is used in the $RO_2 + NO/NO_3$ reactions (Rollins et al., 2009) (Pathway III in Fig. 1b). The $RO_2 + HO_2$ reaction (Pathway I in Fig. 1b) yields a nitrooxy-hydroperoxide (NISOPOOH). For $RO_2 + RO_2$ reactions (Pathway II in Fig. 1b), a branching ratio of 50 % is assumed for the radical propagating pathway versus carbonyl (NIT1) and alcohol (ISOPN) formation reactions. The subsequent oxidation of NIT1 by NO_3 largely follows Rollins et al. (2009), using a reaction rate coefficient of 7.0×10^{-14} cm^3 mol^{-1} s^{-1}, which is about an order of magnitude slower than that of isoprene + NO_3 reactions. Reaction of NIT1 with O_3 is also included, and the reaction rate coefficient (2.5×10^{-17} cm^3 mol^{-1} s^{-1}) is estimated by scaling the NIT1 + NO_3 reaction rate coefficient using methacrolein as a reference compound. Products from NIT1+O_3 reactions and the NIT1+OH oxidation scheme are estimated, largely based on the SAPRC mechanism generation system. The IS mechanism assumes 70 % NO_x recycling efficiency from NIT1 + O_3 oxidation. NIT1 is estimated to react rapidly with OH ($k_{OH} = 3.0 \times 10^{-11}$ cm^3 mol^{-1} s^{-1}), with the reaction having a large yield of propanone nitrate (PROPNNB) and releasing little NO_x. NISOPOOH is treated following Paulot et al. (2012), which assumes its fate is similar to that of hydroxyhydroperoxide formed from isoprene+OH reactions.

While the chemistry simulation maintains the specificity described above, our discussion of the results groups isoprene nitrates as first-generation products (ING_0, including δ- and β-hydroxynitrates, C5-nitrooxycarbonyl, and C5-nitrooxyhydroperoxide) and secondary isoprene nitrates (ING_1 and ING_2), as in Paulot et al. (2012). ING_1 represents

short-lived species, including methyl vinyl ketone nitrate, methacrolein nitrate, ethanal nitrate, and a general isoprene nitrate species (RNO_3I). ING_2 represents propanone nitrate, as it is substantially longer-lived. We use Henry's law constants of $H_{298} = 1.7 \times 10^4\,M\,atm^{-1}$ for ING_0 and ING_1 (von Kuhlmann et al., 2003; Ito et al., 2007) and $H_{298} = 10^3\,M\,atm^{-1}$ for ING_2 (Sander, 1999).

In addition to the changes in isoprene nitrate chemistry, isoprene oxidation chemistry under low-NO_x conditions is updated. In the standard SAPRC-07 mechanism, the low-NO_x oxidation of isoprene is represented by the formation of lumped organic hydroperoxides (R6OOH) from the RO_2+HO_2 pathway.

Here we represent isoprene hydroperoxides explicitly, with updated chemistry including epoxides formation and recycling of OH (Paulot et al., 2009b) (Pathway I in Fig. 1a). Formation of MVK/MACR (12 %) under low-NO_x conditions is attributed to a radical channel in the $ISOPO_2+HO_2$ reaction (Paulot et al., 2009b). We also incorporate isoprene peroxy radical isomerization reactions and subsequent OH-reformation from hydroperoxy-aldehydes (HPALD) (Peeters et al., 2009; Peeters and Müller, 2010) (Pathway II in Fig. 1a). The measured isomerization rate from Crounse et al. (2011) is used, which is ~ 50 times slower than that predicted from theoretical calculations (Peeters et al., 2009; Peeters and Müller, 2010).

Additional changes in the mechanism include revised reaction rates for RO_2+HO_2. The reaction rate coefficient in the base SAPRC-07 mechanism is independent of the size of the peroxy radical:

$$k = 3.80\times10^{-13}\exp(900/T). \quad (1)$$

In fact, k increases with the size of the peroxy radical (Rowley et al., 1992; Jenkin and Hayman, 1995; Boyd et al., 2003), and we use the expression derived by Saunders et al. (2003):

$$k = 2.91\times10^{-13}\exp(1300/T)\left[1-\exp(-0.245n)\right] \quad (2)$$

where n is the number of atoms of carbon in the peroxy radical. For isoprene peroxy radicals, this increases the reaction rate by a factor of 2 at 298 K.

2.2 CMAQ model

CMAQ model version 4.7 is used for photochemical air quality modeling. The inputs to CMAQ are the anthropogenic emissions and meteorological conditions; outputs are concentrations and deposition fluxes for each hour of the simulation. CMAQ employs an Eulerian grid structure to explicitly simulate biogenic emissions, gas-phase, aqueous, and mixed-phase chemistry, advection and dispersion, aerosol thermodynamics and physics, and wet and dry deposition. A more complete description and evaluation of the CMAQ processes and inputs are available in Foley et al. (2010), Carlton et al. (2010), and Appel et al. (2011). CMAQ with the base SAPRC-07T mechanism has been shown to reliably simulate atmospheric concentrations of ozone and aerosols (Hutzell et al., 2012).

The spatial domain covers the entire continental US and a portion of Canada and Mexico. The model includes 24 vertical layers at 36 km horizontal resolution. Chemical boundary conditions are based on the default vertical profiles of gaseous species and aerosols in CMAQ that represent clean air conditions. The model simulation period is 00:00 UTC 1 July to 00:00 UTC 16 August 2004, with the first 96 hours discarded as spin-up to remove the impact of initial conditions.

We use 3-D meteorology fields developed by the 5th Mesoscale Meteorological model (MM5; Grell et al., 1994) version 3.7.4 to drive the photochemical model. The area, onroad mobile, non-road mobile, and point emissions are processed using the Sparse Matrix Operator Kernel Emissions (SMOKE, Houyoux et al., 2000) based on US EPA 2002 National Emission Inventory (NEI) version 3 (http://www.epa.gov/ttn/chief/net/2002inventory.html). Year specific updates for 2004 are included for major power plants and vehicle emissions. We adjust all NO_x emissions (reduce by 20 %), as Napelenok et al. (2008) suggests reduced NO_x emissions are in better agreement with satellite NO_2 measurements for the southeastern United States. For biogenic emissions, studies have found isoprene emissions estimated by the two widely used models, i.e., the Model of Emissions of Gases and Aerosols from Nature (MEGAN) and the Biogenic Emission Inventory System (BEIS), differ by about a factor of 2 (Warneke et al., 2010; Carlton and Baker, 2011). Model predictions compared with measurements during a July 1998 intensive field campaign in the Ozarks find that MEGAN tends to overpredict isoprene emissions, while BEIS shows underpredictions (Carlton and Baker, 2011). To account for the potential underestimation from BEIS, we increase the isoprene emissions calculated by BEIS version 3 (BEIS3) by 50 %.

The treatment of biogenic secondary organic aerosol (SOA) formation follows that in CMAQv4.7 (Carlton et al., 2010). Biogenic SOA formation from gas-phase oxidation of isoprene, monoterpenes, and sesquiterpenes is represented. Isoprene SOA is formed exclusively by OH oxidation. The yield from isoprene semivolatile products and their partitioning parameters are based on the low-NO_x experimental results of Kroll et al. (2006). Monoterpene and sesquiterpene SOA is formed by OH, NO_3, and O_3 oxidation, with the partitioning parameters based on the experimental data of Griffin et al. (1999). Nonvolatile SOA formation including acid enhanced isoprene SOA (Surratt et al., 2007) is also accounted for in the model.

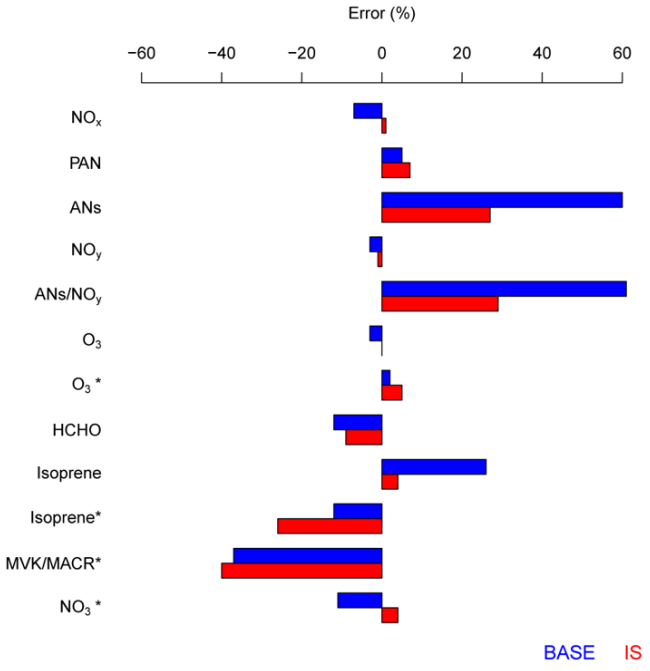

Fig. 2. Evaluation of CMAQ using observations between the surface and 2 km (10–18 LST, except NO_3 is 21–04 LST). *indicates data from WP-3D. HCHO is based on the average of the University of Rhode Island and NCAR measurements due to the systematic difference (∼ 35 %) between the two datasets. The CMAQ model results are sampled at the GPS location of the 1 min measurements. Error is reported the median of the quantity CMAQ minus observations, divided by the median of the observations.

2.3 Observational datasets

We use data from the INTEX-NA/ICARTT campaigns in the summer of 2004 (1 July to 15 August) (Singh et al., 2006; Fehsenfeld et al., 2006) to evaluate model performance and constrain the uncertainties in the isoprene nitrate chemistry. Observations are available from NASA DC-8 and NOAA WP-3D (18 flights on each aircraft). The two aircrafts have different sampling emphasis, with DC-8 targeted at regional airmasses over North America and WP-3D aimed at local flows downwind of urban centers and point sources in the northeastern United States (Fig. 3). During INTEX-NA/ICARTT, the total alkyl and multifunctional nitrates (∑ANs) are measured by thermal dissociation laser induced fluorescence (TD-LIF, Day et al., 2002). The dataset represents the most spatially extensive measurements of ∑ANs over the eastern United States to date. While ∑ANs includes isoprene nitrates (ING), the ∑ANs measurement also includes other organic nitrates as well. As mentioned, these same data have been used in previous studies investigating the formation and fate of isoprene nitrates (Horowitz et al., 2007; Perring et al., 2009a).

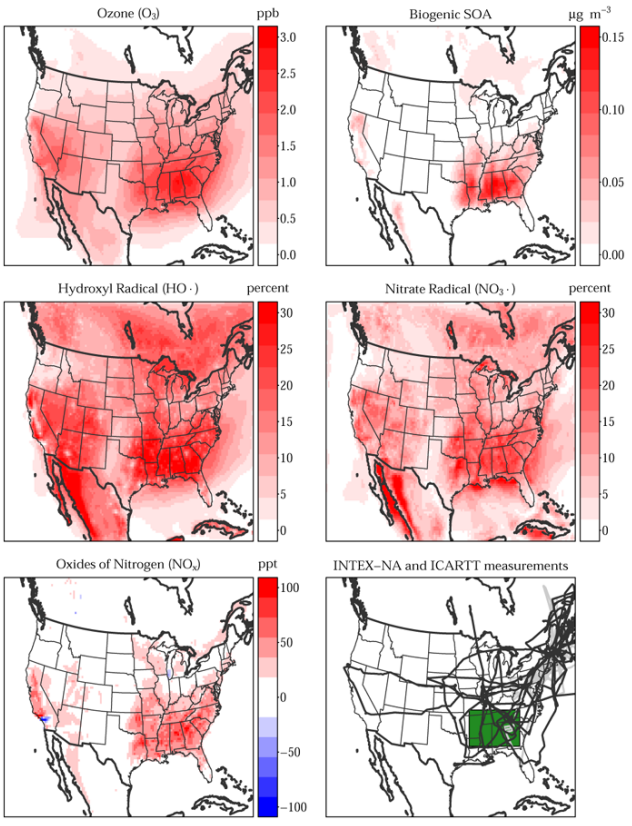

Fig. 3. Changes in the surface concentrations of selected model species between the base and IS simulations averaged over the entire modeling period. DC-8 and WP-3D flight tracks are shown in dark grey and light grey, respectively. The green box indicates the southeastern United States subdomain described in the Results section.

3 Results

3.1 Evaluation of IS mechanism with INTEX-NA/ICARTT observations

With the updated isoprene nitrate chemistry, the IS simulation shows improved performance over a range of species measured by aircraft during the INTEX-NA/ICARTT 2004 field study. Model performance of selected species within the boundary layer is summarized in Fig. 2.

Isoprene nitrates (ING) and ∑ANs are substantially shorter-lived in the IS scheme (Table 2). As a result, ∑ANs concentrations decrease by 20 %, reducing the bias from 60 % to 30 %. NO_x concentrations are slightly underestimated in the base case (−7 %), and have little bias (1 %) in the IS case. The increase in NO_x is due to shorter photochemical lifetime of isoprene nitrates and reduced net removal of NO_x by isoprene nitrate chemistry. HNO_3 (not shown) is biased low in both cases (−44 % for the base, −33 % for IS scheme). For PAN and NO_y ($NO_y = NO_x + \sum PNs + \sum ANs + HNO_3 +$ minor species), both model runs

Table 2. NO_x recycling efficiency and isoprene nitrates lifetime from the base case, IS scheme, and its sensitivity simulations. The isoprene nitrates (ING) are a subset of the alkyl and multifunctional nitrates (ANs).

Name	Description	ING_0 recycling of NO_x (α)	Daytime lifetime (h)		Nighttime lifetime (h)	
			$\sum$ANs	ING	$\sum$ANs	ING
base	base	29 %	13		121	
IS	IS	29 %	7.7	6.1	44	31
A1	day 100 % NO_x	71 %	5.9	3.5	30	16
A2	day 100 % ING	8 %	10	9.7	58	48
B1	night 100 % NO_x	57 %	6.4	4.3	35	23
B2	night 100 % ING	21 %	8.5	7.3	72	62
C	fast deposition	29 %	6.4	4.2	40	26
D	low ING yield	28 %	8.1	6.3	43	29
E	slow HO_2+RO_2	33 %	7.4	5.9	41	30

show good agreement with observations (bias within 7 % for PAN, and within −3 % for NO_y). Observations suggest $\sum$ANs are important components of NO_y (13 %). The base case substantially overestimates the $\sum$ANs : NO_y ratio, whereas the IS simulation reduces the bias by about a factor of 2. Corresponding to the increase in NO_x concentrations, O_3 levels increase slightly (1–2 ppbv) in the IS simulation and both model runs agree well with observed concentrations (bias within ±5 %).

Isoprene concentrations from the DC-8 measurements are slightly overestimated by the base case (bias of 26 %), whereas the IS case shows very little bias (4 %). For measurements from the WP-3D, slight underestimations are found in both runs (−12 % from the base, −26 % from IS). The decreases in isoprene concentrations in the IS case can be related to the increase in OH (∼ 30 %, as shown below). Oxidation products from isoprene, methyl-vinyl ketone (MVK) and methacrolein (MACR) are also measured by the WP-3D flights. Modeled MVK and MACR are well correlated with observations ($R^2 = 0.66$), however both simulations underpredict the concentrations of these species by 40 %. Underestimation of MVK and MACR could be partly attributed to the bias in isoprene, while errors in modeled OH concentrations might cause additional underpredictions of these isoprene oxidation products. Formaldehyde (HCHO) increases slightly (4 %) in the IS case, and both simulations show some underpredictions (bias from base case = −12 %, and bias from IS = −9 %).

For radical species, NO_3 increases by 35 % as a result of increased NO_x and O_3, and the simulation shows good agreement with observations (bias of 4 %). Concentrations of OH increase by 30 %, with the bias improved from −30 % in the base simulation to about −20 % in the IS case. Performance of HO_2 also improves slightly with bias reduced from about −30 % to −25 %. A recent study suggests the traditional OH measurements made by laser-induced fluorescence (LIF) using the Penn State Ground-based Tropospheric Hydrogen Oxides Sensor (used in 2004 INTEX-NA/ICARTT study) tend to overestimate the concentrations due to internally generated OH, likely from oxidation from biogenic VOCs (Mao et al., 2012). It is also reported that HO_2 measured by LIF is likely subject to interference by RO_2 from isoprene, alkenes, or aromatics (Fuchs et al. 2011). Therefore, caution should be taken when interpreting OH and HO_2 performance, especially when biogenic VOCs are abundant. We find the increase in CMAQ simulated HO_x is partly driven by their increased production. The change is related to a number of sources: rapid photolysis of HPALD, increased photolysis from the increase of O_3, and increased photolysis from the increased abundance of isoprene oxidation products (e.g., glyoxal and methylglyoxal). Meanwhile, the changes in NO_x due to updates in isoprene nitrate chemistry further increase OH concentrations by shifting the partitioning between HO_2 and OH through HO_2+NO reaction.

Above the planetary boundary layer in the free troposphere, the impact of the more detailed isoprene chemistry is smaller (Fig. S1). Furthermore, the model underestimates ozone and NO_y in the free troposphere, potentially due to errors in vertical mixing or boundary conditions. Because of these biases and because the short lifetime of isoprene means that relatively little is transported to the free troposphere, we restrict our analysis to concentrations within the planetary boundary layer, where the impact of these biases are reduced.

Changes in modeled surface concentrations of selected species from the IS simulation compared to the base case are shown in Fig. 3. NO_x concentrations increase over extended regions of the continent, with a maximum increase of 40–80 pptv (4 %) over the southeastern US and California where there are abundant isoprene emissions. In contrast to the increase of NO_x in isoprene rich regions, decreases are found in urban areas with very high NO_x but relatively low isoprene concentrations (e.g., Los Angeles). In these urban locations, OH concentrations increase as a result of increased O_3 levels,

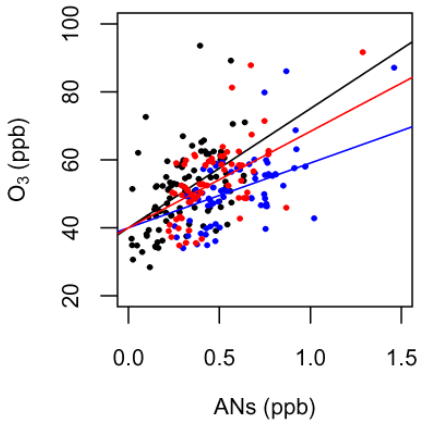

Fig. 4. Observed and simulated relationship between O_3 and $\sum$ANs. Black circles are the daytime observations (11–19 LST) within 2 km of the surface and with isoprene concentration greater than 500 pptv. The blue and red circles are values from the base and IS simulations, respectively, sampled at the location and time of measurements. The black line is the best fit of observations (slope = 35.1, intercept = 40.0, $R^2 = 0.24$, p value = 4.05×10^{-7}). The blue line is the best fit for the base simulation (slope = 19.1, intercept fixed at 40.0, squared correlation coefficient of 0.33, p value: $< 2.2 \times 10^{-16}$), and the red line is the best fit for the IS simulation (slope = 28.4, intercept fixed at 40.0, squared correlation coefficient of 0.33, p value: $< 2.2 \times 10^{-16}$).

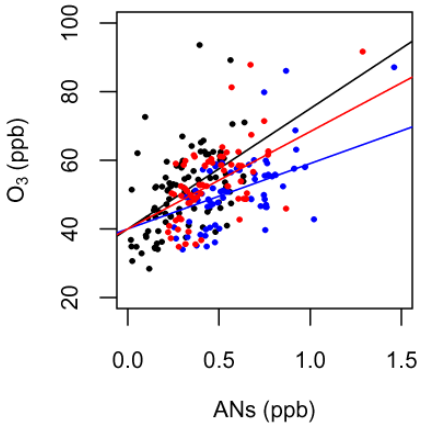

Fig. 5. Simulated fate of isoprene peroxy radicals in the IS and E (slow HO_2+RO_2) cases. Results are averaged over the entire modeling period for the southeastern US within 2 km of the surface. $ISOPO_2$ refers to isoprene peroxy radicals formed from isoprene+OH reactions (Fig. 1a), and $NISOPO_2$ refers to those formed from isoprene+NO_3 reactions (Fig. 1b).

causing more rapid formation of HNO_3 and therefore a decrease in NO_x.

Corresponding to the increase in NO_x concentrations, O_3 levels increase by up to 3 ppbv with the spatial pattern correlated well with the changes in NO_x. Concentrations of OH, HO_2 (not shown), and NO_3 radical also increase by $\sim$30 %, $\sim$6 %, and $\sim$20 % respectively at these locations. With the increases in oxidants levels (OH, O_3, NO_3), biogenic SOA is increased by $\sim$0.1 μg/m^3 (i.e., 10–20 %) in the southeastern United States. We find greater changes when averaging within the boundary layer (<2 km) for the southeastern US: NO_x, 9 %; HO_2, 11 %; and NO_3, 67 %.

We further evaluate model performance using the correlation of O_3 versus $\sum$ANs (Fig. 4) as measured during INTEX-NA/ICARTT. Both are produced from RO_2 reactions with NO, and therefore might provide useful information regarding the $\sum$ANs formation and fate. We restrict our analysis to samples with high isoprene concentrations (> 500 pptv) to focus on isoprene rich air masses. Using linear regression, the observations are fit to a line with slope of 35.1±6.4 ppbv($\sum$AN)/ppbv(O_3). We find observed $\sum$ANs and O_3 are correlated with R^2 of 0.24. The slope is in good agreement with reported morning values at Granite Bay, CA (Cleary et al., 2005), and between the morning and afternoon values found at La Porte, TX (Rosen et al., 2004). Horowitz et al. (2007) use the entire INTEX-NA/ICARTT summer 2004 dataset and find that observations of O_3 versus $\sum$ANs are only weakly correlated ($R^2 = 0.12$) with slope of 81.7. Compared to the correlation and slope reported by Horowitz et al. (2007), we find slightly stronger correlation and reduced slope (a factor of 2) using observations coincident with high isoprene concentrations. Following the methods of Rosen et al. (2004) and Cleary et al. (2005), the slope of 35.1 implies a $\sum$ANs yield of 5.7 %. As the high isoprene observations are mostly found in the afternoon hours, it is expected that this net yield is lower than the actual yield, as some ANs are lost over the course of a day to deposition and photochemistry. Similar findings have been reported by Horowitz et al. (2007), where the inferred yield was about a factor of 2 lower than the isoprene nitrate yield from OH initiated chemistry.

The CMAQ simulated correlations of O_3 versus $\sum$ANs are compared with the observed relationship in Fig. 4. In comparison to the base simulation, the IS scheme greatly reduces the bias relative to the observed slope (−19 % vs. −46 %). Slightly stronger correlations are found in the two model simulations (squared correlation coefficient of 0.33) compared to those from the observations.

In our analysis of O_3 versus $\sum$ANs correlations, the model predicts about 40 % $\sum$ANs from sources other than isoprene (not shown). Prior measurements have inferred a substantial contribution of isoprene to $\sum$ANs (Perring et al., 2009a; Beaver et al., 2012). Additional measurements of speciated organic nitrates are needed to better constrain the contribution of isoprene to the composition of $\sum$ANs.

The IS mechanism with comprehensive isoprene chemistry more accurately simulates observed $\sum$AN, O_3, and NO_x. Nevertheless, substantial uncertainty remains in isoprene nitrate chemistry. In the following sections, we use observations to investigate and constrain these uncertainties.

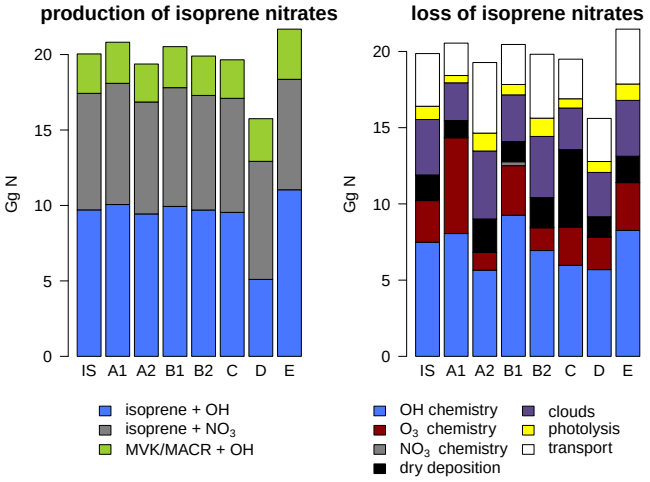

Fig. 6. Simulated production and loss processes for isoprene nitrates from the IS simulation and its sensitivity cases (listed in Table 2). Results are summarized over the entire modeling period for the southeastern US within 2 km of the surface.

Our examination of the isoprene peroxy radical fate and the sources and sinks of isoprene nitrates uses the IS simulation as a reference calculation to obtain a better understanding of the key processes.

3.2 Fate of isoprene peroxy radicals

To quantify the fate of isoprene peroxy radicals, we attribute the sinks to each chemical pathway using the CMAQ model results aggregated between the surface and 2 km in altitude and over the southeastern US. The results are shown in Fig. 5. For the peroxy radicals produced from OH reactions ($ISOPO_2$), the IS simulation suggests primary reactions with Pathway III, NO (44 %) and Pathway I, HO_2 (40 %). Isomerization plays a less important role (9 %) than reported in some previous studies (Peeters et al., 2009; Peeters and Müller, 2010; Archibald et al., 2010; Stavrakou et al., 2010), as we use the rate measured by Crounse et al. (2011). The $RO_2 + HO_2$ reaction pathway has important implications as the epoxides formed from isoprene hydroxyhydroperoxide oxidation have been shown to be an important gas-phase precursor of SOA (Paulot et al., 2009b; Surratt et al., 2010; Froyd et al., 2010; Lin et al., 2012).

For peroxy radicals from NO_3 reactions ($NISOPO_2$), the model predicts their fate is dominated by reactions with Pathway I, HO_2 (43 %) and Pathway II, RO_2 (35 %, including $NISOPO_2$ self-reactions (6 %), and their reactions with methyl peroxy radical (9 %), acetyl peroxy radical (8 %), and a peroxy radical operator (RO2C) (12 %)). The remaining portion is composed of reactions with Pathway III: NO (16 %) and NO_3 (7 %). The dominance of reaction of $NISOPO_2$ with HO_2 is consistent with the laboratory and modeling results from Rollins et al. (2009) and can have significant impacts on the nighttime oxidants levels, as a recent study (Kwan et al., 2012) suggests a large yield (50 %) of OH formation from this pathway (not included in this study). Furthermore, recent laboratory work suggests that NISOPO2 self-reactions may form lower-volatility dimers that contribute to SOA (Ng et al., 2008; Kwan et al., 2012). In our simulation of the southeastern US, six percent of the NISOPO2 radicals undergo self reactions, which suggests this may be a relevant source of SOA but it is not a large sink of NISOPO2. It should be noted, however, that there are large uncertainties in the $RO_2 + RO_2$, $RO_2 + HO_2$, $RO_2 + NO$, and $RO_2 + NO_3$ reaction rates (Orlando and Tyndall, 2012), and better constraints from laboratory and field studies are needed to confirm the relative importance of these pathways.

3.3 Production and loss of isoprene nitrates

Using the same averaging domain over the southeastern US described in Sect. 3.2, the production and loss of isoprene nitrates are shown in Fig. 6 and Table 2. Modeling results from the IS case suggest a large fraction ($\sim$ 40 %) of isoprene nitrates production occurs from isoprene oxidation by NO_3, and subsequent reactions with NO, NO_3, HO_2, and RO_2. This branching ratio of sources from NO_3 oxidation is generally consistent with the findings ($\sim$ 50 %) from Horowitz et al. (2007); however, direct evidence for enhanced formation from this pathway is rare. Ambient observations have been largely limited to mono-functional alkyl nitrates and total alkyl nitrates (Buhr et al., 1990; Flocke et al., 1998; Rosen et al., 2004; Cleary et al., 2005; Day et al., 2009). Only in a few cases the diurnal profiles of specific individual multifunctional organic nitrates have been quantified (Grossenbacher et al., 2001, 2004; Beaver et al., 2012). More ambient measurements are needed to verify model predictions.

For the loss of total isoprene nitrates (ING), we count photochemical reactions as a loss process only if isoprene nitrates are converted to species that no longer retain the nitrate functional group. The model results show that ING loss is dominated by photooxidation by OH (38 %) and O_3 (14 %). O_3 plays a less important role than OH despite reacting rapidly with isoprene nitrates (Lockwood et al., 2010), reflecting the lower NO_x recycling efficiency we assumed in O_3+ISOPN reactions ($\sim$ 30 % in O_3+ISOPN versus $\sim$ 60 % in OH + ISOPN reactions). The additional loss consists of dry deposition (8 %) and cloud processes (18 %, i.e., wet deposition and convective mixing), photolysis (4 %), and advection/diffusion out of the modeling subdomain (17 %). The large contribution from photooxidation is consistent with findings by Shepson et al. (1996), Ito et al. (2007), Perring et al. (2009a), and Paulot et al. (2012). In contrast, Horowitz et al. (2007) concludes that dry deposition is the main sink. The discrepancy is partly due to a faster dry deposition velocity (as of HNO_3) used by Horowitz et al. (2007) and the fact that second-generation isoprene nitrates are assumed to be removed only by deposition processes in that study. The

IS simulation also suggests there are large differences in the daytime versus nighttime lifetime of isoprene nitrates; the isoprene nitrates have a longer lifetime at night.

ING_0, ING_1, and ING_2 attribute 16 %, 30 %, and 11 %, respectively, to $\sum$ANs concentrations, with the remaining ($\sim$ 40 %) from sources other than isoprene (Fig. S2, Supplement). Comparing the relative role played by these different generations of isoprene nitrate species (not shown), ING_0 and ING_1 account for about 40 % and 50 % of the total loss of ING (excluding advection/diffusion), respectively. The large contribution from ING_1 is due to its large fraction in the ING composition and also the fact that even though ING_1 is longer-lived than ING_0 (daytime lifetime $\sim$ 6.2 h versus $\sim$ 1.2 h), it is assumed to release NO_x entirely during photooxidation, whereas a significant portion of ING_0 ($\sim$ 70 %) is assumed to maintain the nitrate functional group in its reactions with OH, O_3, and NO_3. Being much longer-lived (daytime lifetime about 18 h) and accounting for a small fraction of ING, ING_2 contributes only 7 % of the total loss, and may play an important role in the transport of NO_x to remote regions and the free troposphere.

3.4 Sensitivity simulations and constraints with INTEX-NA/ICARTT data

In the previous sections, we have shown the peroxy radical fate as well as production and loss of isoprene nitrates from the IS simulation. Here we examine the sensitivity of model results to the most important uncertainties in our current understanding of isoprene nitrate chemistry, including the yield from the OH/NO reaction pathway, NO_x recycling efficiency from ING_0, dry deposition rate, and RO_2+HO_2 reaction rate (Table 2 and Figs. 1, 5, and 6).

3.4.1 Sensitivity simulations

A. Daytime NO_x recycling: when ING_0 reacts with OH, O_3, and NO_3, it is uncertain whether they will maintain the nitrate functional group or release NO_x (Paulson and Seinfeld, 1992; Giacopelli et al., 2005; Paulot et al., 2009a). In the IS simulation, we use the recycling efficiency ($\sim$ 60 %) from Paulot et al. (2009a) for the ISOPN+OH pathway. Since little is known about the recycling efficiency from ISOPN+O_3 reactions and from nitrates formed from isoprene+NO_3 reactions, we derive the likely products largely based on the SAPRC mechanism generation system. We investigate the uncertainty due to recycling efficiency separately for ING_0 formed from the OH and NO_3 pathways. When recycling is completely turned off, we assume an even split in production of ING_1 (represented by RNO3I) and ING_2 (represented by PROPNN/PROPNNB for OH/NO_3 pathways).

When 100 % recycling efficiency is assumed for ING_0 formed from isoprene oxidation by OH (run A1), the overall recycling efficiency increases to $\sim$ 70 %. Isoprene nitrates production increases slightly (4 %) as a result of increased NO_x, and therefore increases in the fraction of the peroxy radicals reacting with NO. The fraction of isoprene nitrates (ING) lost via photooxidation increases from $\sim$ 55 % in the IS simulation to $\sim$ 70 % in the A1 case. Loss through ING_0 increases by about a factor of 2, causing a substantially reduced lifetime of ING ($\sim$ 6 hours to $\sim$ 4 hours during the day). In contrast, when recycling of NO_x is completely turned off for these hydroxy isoprene nitrates (run A2), the overall recycling efficiency is reduced to $\sim$ 10 %. Production of isoprene nitrates decreases slightly ($-$3 %) as a result of decreased NO_x and thus a decrease in the fraction of the peroxy radicals reacting with NO. Loss via dry deposition and clouds becomes comparable to that via photooxidation, with each process accounting for 35–40 % of the total loss of ING. Loss through ING_0 decreases by about a factor of 2, and consequently the lifetime of ING increases to $\sim$ 10 h during the day.

B. Nighttime NO_x recycling: when 100 % recycling of NO_x is assumed for the ING_0 formed from the isoprene oxidation by NO_3 (run B1), the change is generally similar (though smaller) to trends in the simulation examining the daytime recycling efficiency (run A1). When the recycling is completely turned off (run B2), the overall effects on the production and loss are relatively small, as the IS scheme already assumes the nitrates formed from isoprene + NO_3 reactions release little NO_x while reacting with OH and NO_3. The most significant change is found in the lifetime of ING at night, which increases by a factor of 2. Note that we only examine the recycling of NO_x from isoprene nitrates formed exclusively from NO_3 oxidation (C5-nitrooxycarbonyl and C5-nitrooxyhydroperoxide), which accounts for $\sim$ 90 % of isoprene nitrates production at night.

C. Dry deposition: in the IS run, ING_0 and ING_1 use Henry's law constants of $H_{298} = 1.7 \times 10^4\,M\,atm^{-1}$ (Ito et al., 2007) and ING_2 use a value of $H_{298} = 10^3\,M\,atm^{-1}$ (Sander, 1999) to estimate their loss by wet deposition. We assume the dry deposition velocity is equal to that of PAN ($\sim 0.6\,cm\,s^{-1}$ at daytime), which is on the slow side of measured values (Shepson et al., 1996; Farmer and Cohen, 2008). A sensitivity simulation (run C) is conducted to examine the effect of this uncertainty in dry deposition velocity in which we increase the rate to that of HNO_3 ($\sim 3\,cm\,s^{-1}$), considered to be an upper limit. In this simulation, we find that loss of ING via dry deposition increases from 8 % to 26 % of the total. Combined with removal by clouds, the deposition loss (40 %) becomes comparable to that of photooxidation (47 %). The lifetime of ING during the day also drops considerably (to $\sim$ 4 h).

D. Isoprene nitrate yield: with a yield of 12 % from OH/NO reactions and 70 % from NO_3 reactions, the IS simulation finds that about 40 % of isoprene nitrates are produced from the NO_3 pathways. There have been a number of laboratory studies reporting the yield of the OH/NO pathway, as mentioned previously. Holding the yield from the NO_3 pathway constant, we conduct a sensitivity simulation (run D)

with a yield of 6 % from the OH/NO pathway, and this reduces the total production of isoprene nitrates by 20 %. The change also results in increased relative importance of NO_3 pathways, which accounts for half of isoprene nitrates.

E. $RO_2 + HO_2$ reaction rate: in the IS case, the RO_2+HO_2 reaction rates increase with the size of the molecule, consistent with the laboratory measurements (Rowley et al., 1992; Jenkin and Hayman,1995; Boyd et al., 2003). To assess the effects of using a uniform reaction rate for this class of reactions (as has been assumed in numerous previous studies), a sensitivity simulation is conducted where we change the rates to the value used by the base run (about half of the rate used in the IS scheme for isoprene peroxy radicals at 298 K). This change has a significant impact on the relative importance of NO and HO_2 pathways for the peroxy radicals formed by isoprene reacting with OH ($ISOPO_2$). With the reduced rate of HO_2+$ISOPO_2$, NO becomes the dominant channel ($\sim$ 50 %) and HO_2 accounts for only $\sim$ 25 %. As a result, isoprene nitrates production increases by $\sim$ 10 %. For the peroxy radicals ($NISOPO_2$) formed by isoprene reacting with NO_3, the slower RO_2+HO_2 rates switch the relative importance of HO_2 and RO_2 pathways, but the role of NO and NO_3 channels remains generally the same.

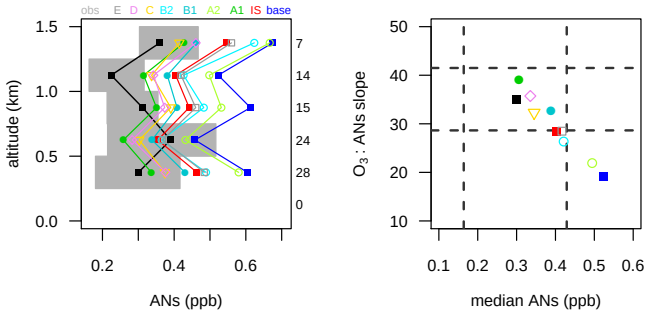

Fig. 7. Modeled and observed vertical profile of $\sum$ANs median concentrations (left) and the slope of the O_3 and $\sum$ANs relationship (right). Data are selected with the same criteria as those in Fig. 4 (daytime observations within 2 km of the surface and with observed isoprene $>$ 500 ppt). Left: The grey boxes show the interquartile ranges of observations. Numbers on the right side of the plot indicate data points in each vertical bin. Right: Uncertainty range of the observations is indicated by horizontal dashed lines (standard error of the fitted slope) and vertical dashed lines (interquartile values of $\sum$ANs). (black square: observation; blue square: base; red square: IS; solid green circle: A1; open green circle: A2; solid blue circle: B1; open blue circle: B2; orange triangle: C; purple diamond: D; grey square: E).

3.4.2 Observational constraints

From previous analysis (Sect. 3.1), we have shown that while the IS simulation has improved model performance for a range of species, there is still notable bias in terms of $\sum$ANs and its correlation with O_3. We also find uncertainties in the isoprene nitrate chemistry have a significant impact on their production and loss processes. Here we use observed $\sum$ANs and O_3 concentrations to further constrain these uncertainties.

In environments with high isoprene concentrations ($>$ 500 pptv), the slope of the correlation between $\sum$ANs and O_3 (Fig. 7) is best mimicked by the simulation with reduced isoprene nitrate yield (run D), while the two 100 % recycling NO_x cases (run A1 and B1) and the fast dry deposition case (run C) also show reasonably good performance and fall within the uncertainty range. On the other hand, the simulation with 0 % NO_x recycling from ING_0 formed from the OH/NO pathway (run A2) substantially degrades the performance, underpredicting the slope by about 40 %.

The simulations that have a slope of $\sum$ANs versus O_3 similar to the observations also show better agreement in terms of $\sum$ANs concentrations. In environments with high isoprene concentrations ($>$ 500 pptv), the IS simulation shows $\sim$ 45 % overestimation of the median $\sum$ANs concentrations, while the base run substantially degrades the model performance with a bias of $\sim$ 90 %. Best agreement is achieved in the runs assuming 100 % recycling of NO_x from ING_0 formed from isoprene oxidation by OH (run A1), using the isoprene nitrate yield of 6 % from the OH/NO pathway (run D), or using a fast dry deposition rate as HNO_3 (run C). When a recycling of 0 % from ING_0 oxidation is assumed (run A2), the agreement substantially worsens with predictions close to the base case. Note that a recent study by Crounse et al. (2012) suggests that methacrolein hydroxy peroxy radicals mostly undergo isomerization and decomposition without forming MACRN in the atmosphere. This, however, should only have minor effects on our conclusions as MACR and MVK together contribute 13–18 % of isoprene nitrates production in the model simulations.

In summary, the base case shows substantial overestimation of $\sum$ANs concentrations and underestimation of the O_3/$\sum$ANs slope. The IS simulation improves both, though it still overpredicts $\sum$ANs by $\sim$ 45 % and underpredicts the O_3/$\sum$ANs slope by 20 %. The NO_x recycling efficiency from ING_0 formed from the OH/NO pathway appears to have the largest impact on the model performance, followed by isoprene nitrate yield, dry deposition rate, and the NO_x recycling efficiency from ING_0 formed from the NO_3 pathway. Improved agreement with the observations can be produced by reducing isoprene nitrate concentrations via any one of the following: (1) using a 6 % yield of isoprene nitrates from the OH/NO pathway; (2) allowing isoprene nitrates to dry deposit as rapidly as HNO_3; (3) assuming a NO_x recycling efficiency of 100 % from ING_0 formed from OH oxidation; or (4) assuming a NO_x recycling efficiency of 100 % from ING_0 formed from NO_3 oxidation. On the other hand, assuming 0 % NO_x recycling from ING_0 formed from OH oxidation shows substantially degraded performance, similar to that of the base run. Note that we evaluate the uncertainties in isoprene nitrate chemistry by varying one parameter

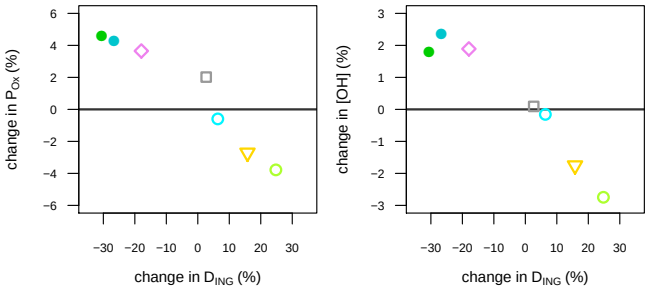

Fig. 8. Correlations between D_{ING} and P_{Ox} (left) and correlations between D_{ING} and OH concentrations (right) from the IS simulation and its sensitivity cases. Results are summarized over the entire modeling period for the southeastern US within 2 km of the surface. Symbols represent the same sensitivity cases as those described in Fig. 7.

at a time, and therefore combinations of changes might further improve the comparison with observations. For example, even though the simulation with 0 % NO_x recycling efficiency for ING_0 formed from NO_3 oxidation shows some underestimation of the $O_3/\sum$ANs slope, it might result in acceptable performance if the isoprene nitrate yield is reduced or a fast dry deposition rate is used. Nevertheless, we find similar daytime lifetimes of isoprene nitrates ($\sim$ 4 h for the 12 % yield cases and $\sim$ 6 h for the 6 % yield case) in both simulations that show good agreement with observations. However, our CMAQ simulation suggests that non-isoprene organic nitrates are 40 % of the $\sum$ANs. Errors in the non-isoprene ANs may influence these results.

3.5 Impacts on OH and Ox

The IS scheme has significant impact on NO_x, NO_3, and biogenic SOA concentrations as compared to the base case. We also find uncertainties in the IS scheme can have large effects on the sources and sinks of isoprene nitrates. Here we further examine the sensitivity of O_3 and OH to these uncertainties in the isoprene nitrate chemistry.

We start our investigation by quantifying the variations in fate of NO_x due to the uncertainties in isoprene nitrate chemistry. Using the methodology of Paulot et al. (2012), the local net removal of NO_x by isoprene nitrates, D_{ING}, is defined as

$$D_{ING} = P_{ING0} + P_{ING1\_new} - L_{ING1} - L_{ING2} - \alpha \times L_{ING0}, \quad (3)$$

where P_{ING0} represents photochemical production of first-generation isoprene nitrates, P_{ING1_new} represents production of isoprene nitrates from MVK and MACR, $\alpha \times L_{ING0}$ represents NO_x recycled from ING_0, and L_{ING1} and L_{ING2} represent photochemical loss of ING_1 and ING_2. Figure 8 shows that changes in O_x(=O_3+ NO_2) production are well correlated with changes in the amount of NO_x removed by isoprene nitrate chemistry (D_{ING}) in the southeastern United States, consistent with the findings of Paulot et al. (2012). The uncertainties in the isoprene nitrate chemistry can impact the production of O_x ($P(O_x)$) by about 10 %, while the sensitivity of $P(O_x)$ to changes in D_{ING} ($\Delta P(O_x)/\Delta D_{ING}$) is about -15 %. The simulation using slower $RO_2 + HO_2$ rates behaves slightly differently from the other models runs, as an increased fraction of RO_2 reacts with NO, and consequently increased O_x production also plays a role. Paulot et al. (2012) studied the effects of these uncertainties in tropical regions (South America, Southeast Asia, and Africa) with a range of NO_x emissions. Compared to their results, we find $\Delta P(O_x)/\Delta D_{ING}$ in our study region is similar to tropical locations which have the highest NO_x emissions, i.e., Southeast Asia or Africa during the biomass burning season. Much greater impact is reported by Paulot et al. (2012) for South America, which is characterized by very low NO and therefore larger ozone production efficiency. Furthermore, the NO_x recycling efficiency from ING_0 appears to have the largest impact on ozone production in our study region, whereas more equally shared importance between deposition velocity, NO_x recycling efficiency, and isoprene nitrate yield is indicated by the results of Paulot et al. (2012) for South America. The differences are likely a result of higher OH and O_3 concentrations, and therefore increased importance of photochemical loss in our study area.

Changes in OH concentrations are also well correlated with changes in D_{ING}, and the uncertainties in isoprene nitrate chemistry can impact OH concentrations by $\sim$ 6 %. The results show OH concentrations generally increase as D_{ING} decreases. However, further reduction of D_{ING} also increases the formation of HNO_3 by reaction of NO_2+OH, which removes NO_x and OH simultaneously (case A1). Compared to the changes from the base to the IS scheme ($\sim$ 30 %), we find less of an impact on OH due to the uncertainties in isoprene nitrate chemistry. This is because the increase in OH in the IS scheme is primarily driven by increased HO_x production rather than changes in NO_x.

4 Conclusions

Air quality in the southeastern United States is influenced by the interplay between abundant isoprene emissions and anthropogenic pollutants. We incorporate recent advances in our understanding of isoprene oxidation chemistry into the SAPRC-07 chemical mechanism within the CMAQ model, including isoprene nitrates formation and oxidation, epoxide formation, and isoprene peroxy radical isomerization. We use observations from the 2004 INTEX-NA/ICARTT field campaign to evaluate model performance and constrain the uncertainties in the isoprene nitrate chemistry.

We find the new model improves the simulation of the aircraft observations for a range of species. We find that most isoprene nitrates are relatively short-lived and prone to returning NO_x, and thus produce increased NO_x (4–9 %) and O_3 (2 ppbv) in the southeastern US. OH concentrations

increase by ∼ 30 % primarily as a result of increased HO_x production. Laboratory studies have also observed OH reformation from $RO_2 + HO_2$ reactions, with differing yields, depending on the source of peroxy radicals (Hasson et al., 2004; Jenkin et al., 2007; Dillon and Crowley, 2008; Taraborrelli et al., 2012). In this work we have considered OH reformation from isoprene peroxy radicals (Paulot et al., 2009b, Taraborrelli et al., 2012; Liu et al., 2012), but not from acyl peroxy radicals and β-oxo peroxy radicals. Assuming OH yield of up to 50 %, recent modeling work has shown that these reactions increase OH concentrations by 5–40 % (Pugh et al., 2010; Kubistin et al., 2010; Stavrakou et al., 2010; Stone et al., 2011). We would expect an additional increase in OH if this source of OH were included in the IS mechanism.

The increase in oxidants (OH, O_3, and NO_3) causes concentrations of biogenic SOA to increase by 15 %. Future work will integrate the detailed representation of isoprene oxidation described here with recent advances elucidating the chemical origins of isoprene SOA (Surratt et al., 2010; Lin et al., 2012).

HO_2 reactions with isoprene peroxy radical are estimated to account for ∼ 40 % of total reactions during both daytime and nighttime oxidation, highlighting the importance of a better understanding of the oxidation products from this pathway even for a region with elevated NO_x concentrations. The isoprene peroxy radical isomerization accounts for ∼ 10 % of the total.

We examine the sensitivity of our model results to the key assumptions in the isoprene nitrate chemistry, including the yield from the OH/NO pathway, NO_x recycling efficiency from first generation isoprene nitrates, dry deposition rate, and RO_2+HO_2 reaction rates. Constrained by observed $\sum$ANs and their correlation with O_3, reasonably good agreement can be achieved using a range of isoprene nitrate yields and daytime lifetimes: between 6 %, ∼ 6 h and 12 %, ∼ 4 h.

Uncertainties in the isoprene nitrate chemistry can impact ozone production by ∼ 10 % and OH concentrations by ∼ 6 % in the southeastern United States. The effects are well-correlated with the changes in the net amount of NO_x removed by isoprene nitrate chemistry, consistent with findings from Paulot et al. (2012). The uncertainties in NO_x recycling efficiency appear to have a larger impact than uncertainties in isoprene nitrate yield and dry deposition velocity.

We find 40–50 % of the isoprene nitrates are formed from isoprene + NO_3 reactions, consistent with previous findings (Horowitz et al., 2007). Substantial uncertainty exists in the nighttime isoprene nitrate chemistry and peroxy radical fate, and further studies are required to elucidate the oxidation pathways and products. We find that photooxidation accounts for about half of the total loss of isoprene nitrates even when these compounds dry deposit as rapidly as HNO_3. A significant fraction of the loss proceeds via production of secondary oxidation products whose fate remain very uncertain.

In regions at the confluence of biogenic emissions and anthropogenic pollution, accurate simulations of the ozone and secondary organic aerosol depend on representing the isoprene oxidation chemistry accurately. Further progress depends on improved understanding of isoprene oxidation pathways, rate of NO_x recycling from isoprene nitrates, and the fate of the secondary, tertiary, and further oxidation products of isoprene.

Supplementary material related to this article is available online at: http://www.atmos-chem-phys.net/13/8439/2013/acp-13-8439-2013-supplement.pdf.

Acknowledgements. We thank the entire INTEX-NA/ICARTT team for the use of their measurement data. We also thank Barron Henderson, Melinda Beaver, Tad Kleindienst, and John Crounse for helpful conversations. This research was supported by the National Research Council Research Associateship Program pursued at the US Environmental Protection Agency. Fabien Paulot acknowledges support from a NASA Earth and Space Science fellowship. *Disclaimer*: although this article has been reviewed by the EPA and approved for publication, it does not necessarily reflect EPA policies or views.

Edited by: J. Thornton

References

Appel, K. W., Foley, K. M., Bash, J. O., Pinder, R. W., Dennis, R. L., Allen, D. J., and Pickering, K.: A multi-resolution assessment of the Community Multiscale Air Quality (CMAQ) model v4.7 wet deposition estimates for 2002–2006, Geosci. Model Dev., 4, 357–371, doi:10.5194/gmd-4-357-2011, 2011

Archibald, A. T., Cooke, M. C., Utembe, S. R., Shallcross, D. E., Derwent, R. G., and Jenkin, M. E.: Impacts of mechanistic changes on HO_x formation and recycling in the oxidation of isoprene, Atmos. Chem. Phys., 10, 8097–8118, doi:10.5194/acp-10-8097-2010, 2010.

Barnes, I., Bastian, V., Becker, K. H., and Tong, Z.: Kinetics and products of the reactions of NO_3 with monoalkenes, dialkenes, and monoterpenes, J. Phys. Chem., 94, 2413–2419, 1990.

Barnes, I., Becker, K. H., and Tong, Z.: Near UV absorption spectra and photolysis products of difunctional organic nitrates: possible importance as NO_x reservoirs, J. Atmos. Chem. 17, 353–373, 1993.

Beaver, M. R., Clair, J. M. St., Paulot, F., Spencer, K. M., Crounse, J. D., LaFranchi, B. W., Min, K. E., Pusede, S. E., Wooldridge, P. J., Schade, G. W., Park, C., Cohen, R. C., and Wennberg, P. O.: Importance of biogenic precursors to the budget of organic nitrates: observations of multifunctional organic nitrates by CIMS and TD-LIF during BEARPEX 2009, Atmos. Chem. Phys., 12, 5773–5785, doi:10.5194/acp-12-5773-2012, 2012.

Berndt, T. and Boge, O.: Gas-phase reaction of NO_3 radicals with isoprene: A kinetic and mechanistic study, Int. J. Chem. Kinet., 29, 755–765, 1997.

Boyd, A. A., Flaud, P.-M., Daugey, N., and Lesclaux, R.: Rate constants for RO_2 + HO_2 reactions measured under a large excess of HO_2, J. Phys. Chem. A, 107, 818–821, doi:10.1021/jp026581r, 2003.

Brown, S. S., deGouw, J. A., Warneke, C., Ryerson, T. B., Dubé, W. P., Atlas, E., Weber, R. J., Peltier, R. E., Neuman, J. A., Roberts, J. M., Swanson, A., Flocke, F., McKeen, S. A., Brioude, J., Sommariva, R., Trainer, M., Fehsenfeld, F. C., and Ravishankara, A. R.: Nocturnal isoprene oxidation over the Northeast United States in summer and its impact on reactive nitrogen partitioning and secondary organic aerosol, Atmos. Chem. Phys., 9, 3027–3042, doi:10.5194/acp-9-3027-2009, 2009.

Buhr, M. P., Parrish, D. D., Norton, R. B., Fehsenfeld, F. C., Sievers, R. E., and Roberts, J. M.: Contribution of organic nitrates to the total reactive nitrogen budget at a rural eastern US site, J. Geophys. Res., 95, 9809–9816, 1990.

Butler, T. M., Taraborrelli, D., Brühl, C., Fischer, H., Harder, H., Martinez, M., Williams, J., Lawrence, M. G., and Lelieveld, J.: Improved simulation of isoprene oxidation chemistry with the ECHAM5/MESSy chemistry-climate model: lessons from the GABRIEL airborne field campaign, Atmos. Chem. Phys., 8, 4529–4546, doi:10.5194/acp-8-4529-2008, 2008.

Byun, D. and Schere, K. L.: Review of the governing equations, computational algorithms, and other components of the Models-3 Community Multiscale Air Quality (CMAQ) modeling system, Appl. Mech. Rev., 59, 51–77, 2006.

Carlton, A. G. and Baker, K. R.: Photochemical modeling of the Ozark isoprene volcano: MEGAN, BEIS, and their impacts on air quality predictions, Environ. Sci. Technol., 45, 4438–4445, doi:10.1021/es200050x, 2011.

Carlton, A. G., Bhave, P. V., Napelenok, S. L., Edney, E. O., Sarwar, G., Pinder, R. W., Pouliot, G. A., and Houyoux, M.: Model Representation of Secondary Organic Aerosol in CMAQv4.7, Environ. Sci. Technol., 44, 8553–8560, 2010.

Carter, W. P. L.: Documentation of the SAPRC-99 Chemical Mechanism for VOC Reactivity Assessment, Final report to the California Air Resources Board, Contracts 92–329 and 95–308, 8 May 2000 (available at: http://www.cert.ucr.edu/~carter/absts.htm{#}saprc99), 2000.

Carter, W. P. L.: Development of the SAPRC-07 Chemical Mechanism, Atmos. Environ., 44, 5324–5335, 2010a.

Carter, W. P. L.: Development of the SAPRC-07 chemical mechanism and updated ozone reactivity scales, Report to the California Air Resources Board, Contract No. 03–18, 06-408, and 07-730, 27 January 2010b (available at: http://www.engr.ucr.edu/~carter/SAPRC/), 2010b.

Chen, X., Hulbert, D., and Shepson, P. B.: Measurement of the organic nitrate yield from OH reaction with isoprene, J. Geophys. Res., 103, 25563–25568, doi:10.1029/98JD01483, 1998.

Chuong, B. and Stevens, P. S.: Measurements of the kinetics of the OH-initiated oxidation of isoprene, J. Geophys. Res., 107, 4162, doi:10.1029/2001JD000865, 2002.

Claeys, M., Graham, B., Vas, G.,Wang,W., Vermeylen, R., Pashynska, V., Cafmeyer, J., Guyon, P., Andreae, M. O., Araxo, P., and Maenhaut, W.: Formation of secondary organic aerosols through photooxidation of isoprene, Science, 303, 1173–1176, 2004.

Cleary, P. A., Murphy, J. G., Wooldridge, P. J., Day, D. A., Millet, D. B., McKay, M., Goldstein, A. H., and Cohen, R. C.: Observations of total alkyl nitrates within the Sacramento Urban Plume, Atmos. Chem. Phys. Discuss., 5, 4801–4843, doi:10.5194/acpd-5-4801-2005, 2005.

Crounse, J. D., Paulot, F., Kjaergaard, H. G., and Wennberg, P. O.: Peroxy radical isomerization in the oxidation of isoprene, Phys. Chem. Chem. Phys., 13, 13607–13613, doi:10.1039/c1cp21330j, 2011.

Crounse, J. D., Knap, H. C., Ørnsø, K. B., Jørgensen, S., Paulot, F., Kjaergaard, H. G., and Wennberg, P. O.: Atmospheric fate of methacrolein. 1. Peroxy radical isomerization following addition of OH and O_2, J. Phys. Chem. A, 116, 5756–5762, doi:10.1021/jp211560u, 2012.

Day, D. A., Wooldridge, P. J., Dillon, M. B., Thornton, J. A., and Cohen, R. C.: A thermal dissociation laser-induced fluorescence instrument for in situ detection of NO_2, peroxy nitrates, alkyl nitrates, and HNO_3, J. Geophys. Res., 107, 4046, doi:10.1029/2003JD003685, 2002.

Day, D. A., Farmer, D. K., Goldstein, A. H., Wooldridge, P. J., Minejima, C., and Cohen, R. C.: Observations of NO_x, ΣPNs, ΣANs, and HNO_3 at a Rural Site in the California Sierra Nevada Mountains: summertime diurnal cycles, Atmos. Chem. Phys., 9, 4879–4896, doi:10.5194/acp-9-4879-2009, 2009.

Dillon, T. J. and Crowley, J. N.: Direct detection of OH formation in the reactions of HO_2 with $CH_3C(O)O_2$ and other substituted peroxy radicals, Atmos. Chem. Phys., 8, 4877–4889, doi:10.5194/acp-8-4877-2008, 2008.

Edney, E. O., Kleindienst, T. E., Jaoui, M., Lewandowski, M., Offenberg, J. H.,Wang,W., and Claeys, M.: Formation of 2-methyl tetrols and 2-methylglyceric acid in secondary organic aerosol from laboratory irradiated isoprene/NO_x/SO_2/air mixtures and their detection in ambient $PM_{2.5}$ samples collected in the eastern United States, Atmos. Environ., 39, 5281–5289, 2005.

Farmer, D. K. and Cohen, R. C.: Observations of HNO_3, ΣAN, ΣPN and NO_2 fluxes: evidence for rapid HO_x chemistry within a pine forest canopy, Atmos. Chem. Phys., 8, 3899–3917, doi:10.5194/acp-8-3899-2008, 2008.

Fehsenfeld, F. C., Ancellet, G., Bates, T. S., Goldstein, A. H., Hardesty, R. M., Honrath, R., Law, K. S., Lewis, A. C., Leaitch, R., McKeen, S., Meagher, J., Parrish, D. D., Pszenny, A. A., Russell, P. B., Schlager, H., Seinfeld, J., Talbot, R., and Zbinden, R.: International Consortium for Atmospheric Research on Transport and Transformation (ICARTT): North America to Europe – Overview of the 2004 summer field study, J. Geophys. Res., 111, D23S01, doi:10.1029/2006JD007829, 2006.

Flocke, F., Volz-Thomas, A., Buers, H. J., Patz, W., Garthe, H. J., and Kley, D.: Long-term measurements of alkyl nitrates in southern Germany 1. General behavior and seasonal and diurnal variation, J. Geophys. Res., 103, 5729–5746, 1998.

Foley, K. M., Roselle, S. J., Appel, K. W., Bhave, P. V., Pleim, J. E., Otte, T. L., Mathur, R., Sarwar, G., Young, J. O., Gilliam, R. C., Nolte, C. G., Kelly, J. T., Gilliland, A. B., and Bash, J. O.: Incremental testing of the Community Multiscale Air Quality (CMAQ) modeling system version 4.7, Geosci. Model Dev., 3, 205–226, doi:10.5194/gmd-3-205-2010, 2010.

Froyd, K. D., Murphy, S. M., Murphy, D. M., de Gouw, J. A., Eddingsaas, N. C., and Wennberg, P. O.: Contribution of isoprene-derived organosulfates to free tropospheric aerosol mass, Proc. Nat. Acad. of Science of the USA, 107, 21360–21365, 2010.

Fuchs, H., Bohn, B., Hofzumahaus, A., Holland, F., Lu, K. D., Nehr, S., Rohrer, F., and Wahner, A.: Detection of HO_2 by laser-induced fluorescence: calibration and interferences from RO_2 radicals, Atmos. Meas. Tech., 4, 1209–1225, doi:10.5194/amt-4-1209-2011, 2011.

Giacopelli, P., Ford, K., Espada, C., and Shepson, P. B.: Comparison of the measured and simulated isoprene nitrate distributions above a forest canopy, J. Geophys. Res., 110, D01304, doi:10.1029/2004JD005123, 2005.

Grell, G. A., Dudhia, J., and Stauffer, D. R.: A description of the fifth-generation Penn State/NCAR mesoscale model (MM5), National Center for Atmospheric Research, Boulder, CO, USA, NCAR/TN-398+STR, 122 pp., 1994.

Griffin, R. J., Cocker, D. R., Flagan, R. C., and Seinfeld, J. H.: Organic aerosol formation from the oxidation of biogenic hydrocarbons, J. Geophys. Res., 104, 3555–3567, 1999.

Grossenbacher, J. W., Couch, T., Shepson, P. B., Thornberry, T., Witmer-Rich, M., Carroll, M. A., Faloona, I., Tan, D., Brune,W., Ostling, K., and Bertman, S.: Measurements of isoprene nitrates above a forest canopy, J. Geophys. Res., 106, 24429– 24438, 2001.

Grossenbacher, J. W., Barket, D. J., Shepson, P. B., Carroll, M. A., Olszyna, K., and Apel, E.: A comparison of isoprene nitrate concentrations at two forest-impacted sites, J. Geophys. Res., 109, D11311, doi:10.1029/2003JD003966, 2004.

Guenther, A., Karl, T., Harley, P., Wiedinmyer, C., Palmer, P. I., and Geron, C.: Estimates of global terrestrial isoprene emissions using MEGAN (Model of Emissions of Gases and Aerosols from Nature), Atmos. Chem. Phys., 6, 3181–3210, doi:10.5194/acp-6-3181-2006, 2006.

Hasson, A. S., Tyndall, G. S., and Orlando, J. J.: A product yield study of the reaction of HO_2 radicals with ethyl peroxy ($C_2H_5O_2$), acetyl peroxy ($CH_3C(O)O_2$), and acetonyl peroxy ($CH_3C(O)CH_2O_2$) radicals, J. Phys. Chem. A, 108, 5979–5989, 2004.

Horowitz, L. W., Fiore, A. M., Milly, G. P., Cohen, R. C., Perring, A., Wooldridge, P. J., Hess, P. G., Emmons, L. K., and Lamarque, J.: Observational constraints on the chemistry of isoprene nitrates over the eastern United States, J. Geophys. Res., 112, D01304, doi:10.1029/2006JD007747, 2007.

Houyoux, M. R., Vukovich, J. M., Coats, C. J. Jr., and Wheeler, N. J. M.: Emission inventory development and processing for the Seasonal Model for Regional Air Quality (SMRAQ) project, J. Geophys. Res., 105, 9079–9090, 2000.

Hutzell, W. T., Luecken, D. J., Appel, K. W., and Carter, W. P. L.: Interpreting predictions from the SAPRC07 mechanism based on regional and continental simulations, Atmos. Environ., 46, 417–429, 2012.

Ito, A., Sillman, S., and Penner, J. E.: Effects of additional nonmethane volatile organic compounds, organic nitrates, and direct emissions of oxygenated organic species on global tropospheric chemistry, J. Geophys. Res., 112, D06309, doi:10.1029/2005JD006556, 2007.

Jenkin, M. E. and Hayman, G. D.: Kinetics of reactions of primary, secondary and tertiary beta-hydroxy peroxyl radicals: application to isoprene degradation, J. Chem. Soc., Faraday Trans. 91, 1911–1922, 1995.

Jenkin, M. E., Hurley, M. D., and Wallington, T. J.: Investigation of the radical product channel of the $CH_3C(O)O_2+HO_2$ reaction in the gas phase, Phys. Chem. Chem. Phys., 9, 3149–3162, 2007.

Karl, T., Guenther, A., Turnipseed, A., Tyndall, G., Artaxo, P., and Martin, S.: Rapid formation of isoprene photo-oxidation products observed in Amazonia, Atmos. Chem. Phys., 9, 7753–7767, doi:10.5194/acp-9-7753-2009, 2009.

Kleindienst, T. E., Lewandowski, M., Offenberg, J. H., Jaoui, M., and Edney, E. O.: Ozone-isoprene reaction: Re-examination of the formation of secondary organic aerosol, Geophys. Res. Lett., 34, L01805, doi:10.1029/2006GL027485, 2007.

Kroll, J. H., Ng, N. L., Murphy, S. M., Flagan, R. C., and Seinfeld, J. H.: Secondary organic aerosol formation from isoprene photooxidation, Environ. Sci. Technol., 40, 1869–1877, 2006.

Kubistin, D., Harder, H., Martinez, M., Rudolf, M., Sander, R., Bozem, H., Eerdekens, G., Fischer, H., Gurk, C., Klpfel, T., Knigstedt, R., Parchatka, U., Schiller, C. L., Stickler, A., Taraborrelli, D., Williams, J., and Lelieveld, J.: Hydroxyl radicals in the tropical troposphere over the Suriname rainforest: comparison of measurements with the box model MECCA, Atmos. Chem. Phys., 10, 9705–9728, doi:10.5194/acp-10-9705-2010, 2010.

Kwan, A. J., Chan, A. W. H., Ng, N. L., Kjaergaard, H. G., Seinfeld, J. H., and Wennberg, P. O.: Peroxy radical chemistry and OH radical production during the NO_3-initiated oxidation of isoprene, Atmos. Chem. Phys. Discuss., 12, 2259–2302, doi:10.5194/acpd-12-2259-2012, 2012.

Lelieveld, J., Butler, T. M., Crowley, J. N., Dillon, T. J., Fischer, H., Ganzeveld, L., Harder, H., Lawrence, M. G., Martinez, M., Taraborrelli, D., and Williams, J.: Atmospheric oxidation capacity sustained by a tropical forest, Nature, 452, 737–740, doi:10.1038/nature06870, 2008.

Lin, Y.-H., Zhang, Z., Docherty, K. S., Zhang, H., Budisulistiorini, S. H., Rubitschun, C. L., Shaw, S. L., Knipping, E. M., Edgerton, E. S., and Kleindienst, T. E., Gold, A., and Surratt, J. D.: Isoprene epoxydiols as precursors to secondary organic aerosol formation: acid-catalyzed reactive uptake studies with authentic compounds, Environ. Sci. Technol., 46, 250–258, 2012.

Liu, Y. J., Herdlinger-Blatt, I., McKinney, K. A., and Martin, S. T.: Production of methyl vinyl ketone and methacrolein via the hydroperoxyl pathway of isoprene oxidation, Atmos. Chem. Phys. Discuss., 12, 33323–33358, doi:10.5194/acpd-12-33323-2012, 2012.

Lockwood, A. L., Shepson, P. B., Fiddler, M. N., and Alaghmand, M.: Isoprene nitrates: preparation, separation, identification, yields, and atmospheric chemistry, Atmos. Chem. Phys., 10, 6169–6178, doi:10.5194/acp-10-6169-2010, 2010.

Mao, J., Ren, X., Zhang, L., Van Duin, D. M., Cohen, R. C., Park, J.-H., Goldstein, A. H., Paulot, F., Beaver, M. R., Crounse, J. D., Wennberg, P. O., DiGangi, J. P., Henry, S. B., Keutsch, F. N., Park, C., Schade, G. W., Wolfe, G. M., Thornton, J. A., and Brune, W. H.: Insights into hydroxyl measurements and atmospheric oxidation in a California forest, Atmos. Chem. Phys., 12, 8009–8020, doi:10.5194/acp-12-8009-2012, 2012.

Napelenok, S. L., Pinder, R. W., Gilliland, A. B., and Martin, R. V.: A method for evaluating spatially-resolved NO_x emissions using Kalman filter inversion, direct sensitivities, and space-based NO_2 observations, Atmos. Chem. Phys., 8, 5603–5614, doi:10.5194/acp-8-5603-2008, 2008.

Ng, N. L., Kwan, A. J., Surratt, J. D., Chan, A. W. H., Chhabra, P. S., Sorooshian, A., Pye, H. O. T., Crounse, J. D., Wennberg, P. O., Flagan, R. C., and Seinfeld, J. H.: Secondary organic aerosol

(SOA) formation from reaction of isoprene with nitrate radicals (NO_3), Atmos. Chem. Phys., 8, 4117–4140, doi:10.5194/acp-8-4117-2008, 2008.

Orlando, J. J. and Tyndall, G. S.: Laboratory studies of organic peroxy radical chemistry: an overview with emphasis on recent issues of atmospheric significance, Chem. Soc. Rev., 41, 6294–6317, 2012.

Patchen, A. K., Pennino, M. J., Kiep, A. C., and Elrod, M. J.: Direct kinetics study of the product-forming channels of the reaction of isoprene-derived hydroxyperoxy radicals with NO, Int. J. Chem. Kinet., 39, 353–361, 2007.

Paulot, F., Crounse, J. D., Kjaergaard, H. G., Kroll, J. H., Seinfeld, J. H., and Wennberg, P. O.: Isoprene photooxidation: new insights into the production of acids and organic nitrates, Atmos. Chem. Phys., 9, 1479–1501, doi:10.5194/acp-9-1479-2009, 2009a.

Paulot, F., Crounse, J. D., Kjaergaard, H. G., Kurten, A., St. Clair, J. M., Seinfeld, J. H., and Wennberg, P. O.: Unexpected epoxide formation in the gas-phase photooxidation of isoprene, Science, 325, 730–733, doi:10.1126/science.1172910, 2009b.

Paulot, F., Henze, D. K., and Wennberg, P. O.: Impact of the isoprene photochemical cascade on tropical ozone, Atmos. Chem. Phys., 12, 1307–1325, doi:10.5194/acp-12-1307-2012, 2012.

Paulson, S. and Seinfeld, J.: Development and evaluation of a photooxidation mechanism for isoprene, J. Geophys. Res., 97, 20703–20715, doi:10.1029/92JD01914, 1992.

Peeters, J. and Müller, J.-F.: HO_x radical regeneration in isoprene oxidation via peroxy radical isomerisations. II: experimental evidence and global impact, Phys. Chem. Chem. Phys., 12, 14227–14235, doi:10.1039/C0CP00811G, 2010.

Peeters, J., Nguyen, T., and Vereecken, L.: HO_x radical regeneration in the oxidation of isoprene, Phys. Chem. Chem. Phys., 11, 5935–5939, doi:10.1039/b908511d, 2009.

Perring, A. E., Bertram, T. H., Wooldridge, P. J., Fried, A., Heikes, B. G., Dibb, J., Crounse, J. D., Wennberg, P. O., Blake, N. J., Blake, D. R., Brune, W. H., Singh, H. B., and Cohen, R. C.: Airborne observations of total $RONO_2$: new constraints on the yield and lifetime of isoprene nitrates, Atmos. Chem. Phys., 9, 1451–1463, doi:10.5194/acp-9-1451-2009, 2009a.

Perring, A. E., Wisthaler, A., Graus, M., Wooldridge, P. J., Lockwood, A. L., Mielke, L. H., Shepson, P. B., Hansel, A., and Cohen, R. C.: A product study of the isoprene+NO_3 reaction, Atmos. Chem. Phys., 9, 4945–4956, doi:10.5194/acp-9-4945-2009, 2009b.

Pugh, T. A. M., MacKenzie, A. R., Hewitt, C. N., Langford, B., Edwards, P. M., Furneaux, K. L., Heard, D. E., Hopkins, J. R., Jones, C. E., Karunaharan, A., Lee, J., Mills, G., Misztal, P., Moller, S., Monks, P. S., and Whalley, L. K.: Simulating atmospheric composition over a South-East Asian tropical rainforest: performance of a chemistry box model, Atmos. Chem. Phys., 10, 279–298, doi:10.5194/acp-10-279-2010, 2010.

Ren, X., Olson, J. R., Crawford, J., Brune, W. H., Mao, J., Long, R. B., Chen, Z., Chen, G., Avery, M. A., Sachse, G. W., Barrick, J. D., Diskin, G. S., Huey, L.G., Fried, A., Cohen, R. C., Heikes, B., Wennberg, P. O., Singh, H. B., Blake, D. R., and Shetter, R. E.: HO_x chemistry during INTEX-A 2004: Observation, model calculation, and comparison with previous studies, J. Geophys. Res., 113, 5310, doi:10.1029/2007JD009166, 2008.

Roberts, J. M. and Fajer, R. W.: UV absorption cross sections of organic nitrates of potential atmospheric importance and estimation of atmospheric lifetimes, Environ. Sci. Technol., 23, 945–951, doi:10.1021/es00066a003, 1989.

Rollins, A. W., Kiendler-Scharr, A., Fry, J. L., Brauers, T., Brown, S. S., Dorn, H.-P., Dubé, W. P., Fuchs, H., Mensah, A., Mentel, T. F., Rohrer, F., Tillmann, R., Wegener, R., Wooldridge, P. J., and Cohen, R. C.: Isoprene oxidation by nitrate radical: alkyl nitrate and secondary organic aerosol yields, Atmos. Chem. Phys., 9, 6685–6703, doi:10.5194/acp-9-6685-2009, 2009.

Rosen, R. S., Wood, E. C., Wooldridge, P. J., Thornton, J. A., Day, D. A., Kuster, W., Williams, E. J., Jobson, B. T., and Cohen, R. C.: Observations of total alkyl nitrates during Texas Air Quality Study 2000: Implications for O_3 and alkyl nitrate photochemistry, J. Geophys. Res., 109, D07303, doi:10.1029/2003JD004227, 2004.

Rowley, D. M., Lesclaux, R., Lightfoot, P. D., Noziere, B.,Wallington, T. J., and Hurley, M. D.: Kinetic and mechanistic studies of the reactions of cyclopentylperoxy and cyclohexylperoxy radicals with HO_2, J. Phys. Chem., 96, 4889–4894, 1992.

Sander, R.: Compilation of Henry's Law constants for inorganic and organic species of potential importance in environmental chemistry, version 3, 1999.

Saunders, S. M., Jenkin, M. E., Derwent, R. G., and Pilling, M. J.: Protocol for the development of the Master Chemical Mechanism, MCM v3 (Part A): tropospheric degradation of nonaromatic volatile organic compounds, Atmos. Chem. Phys., 3, 161–180, doi:10.5194/acp-3-161-2003, 2003.

Shepson, P. B., Mackay, E., and Muthuramu, K.: Henry's law constants and removal processes for several atmospheric β-hydroxy alkyl nitrates, Environ. Sci. Technol., 30, 3618–3623, 1996.

Singh, H. B., Brune, W. H., Crawford, J. H., Jacob, D. J., and Russell, P. B.: Overview of the summer 2004 intercontinental chemical transport experiment – North America (INTEX-A), J. Geophys. Res., 111, doi:10.1029/2006JD007905, 2006.

Sprengnether, M., Demerjian, K. L., Donahue, N. M., and Anderson, J. G.: Product analysis of the OH oxidation of isoprene and 1, 3-butadiene in the presence of NO, J. Geophys. Res., 107, 4268, doi:10.1029/2001JD000716, 2002.

Starn, T. K., Shepson, P. B., Bertman, S. B., White, J. S., Splawn, B. G., Riemer, D. D., Zika, R. G., and Olszyna, K.: Observations of isoprene chemistry and its role in ozone production at a semirural site during the 1995 Southern Oxidants Study, J. Geophys. Res., 103, 22425–22435, 1998.

Stavrakou, T., Peeters, J., and Müller, J.-F.: Improved global modelling of HO_x recycling in isoprene oxidation: evaluation against the GABRIEL and INTEX-A aircraft campaign measurements, Atmos. Chem. Phys., 10, 9863–9878, doi:10.5194/acp-10-9863-2010, 2010.

Stavrakou, T., Müller, J.-F., Peeters, J., Razavi, A., Clarisse, L., Clerbaux, C., Coheur, P.-F., Hurtmans, D., De Mazière, M., Vigouroux, C., Deutscher, N. M., Griffith, D. W. T., Jones, N., and Paton-Walsh, C.: Satellite evidence for a large source of formic acid from boreal and tropical forests, Nat. Geosci., 5, 26–30, doi:10.1038/ngeo1354, 2012.

Stone, D., Evans, M. J., Edwards, P. M., Commane, R., Ingham, T., Rickard, A. R., Brookes, D. M., Hopkins, J., Leigh, R. J., Lewis, A. C., Monks, P. S., Oram, D., Reeves, C. E., Stewart, D., and Heard, D. E.: Isoprene oxidation mechanisms: measurements and modelling of OH and HO_2 over a South-East Asian tropical

rainforest during the OP3 field campaign, Atmos. Chem. Phys., 11, 6749–6771, doi:10.5194/acp-11-6749-2011, 2011.

Surratt, J. D., Lewandowski, M., Offenberg, J. H., Jaoui, M., Kleindienst, T. E., Edney, E. O., and Seinfeld, J. H.: Effect of acidity on secondary organic aerosol formation from isoprene, Environ. Sci. Technol., 41, 5363–5369, 2007.

Surratt, J. D., Chan, A. W. H., Eddingsaas, N. C., Chan, M., Loza, C. L., Kwan, A. J., Hersey, S. P., Flagan, R. C., Wennberg, P. O., and Seinfeld, J. H.: Reactive intermediates revealed in secondary organic aerosol formation from isoprene, Proc. Natl. Acad. Sci., 107, 6640–6645, doi:10.1073/pnas.0911114107, 2010.

Taraborrelli, D., Lawrence, M. G., Crowley, J. N., Dillon, T. J., Gromov, S., Gross, C. B. M., Vereecken, L., and Lelieveld, J.: Hydroxyl radical buffered by isoprene oxidation over tropical forests, Nat. Geosci., 5, 190–193, 2012.

Thornton, J. A., Wooldridge, P. J., Cohen, R. C., Martinez, M., Harder, H., Brune,W. H.,Williams, E. J., Roberts, J. M., Fehsenfeld, F. C., Hall, S. R., Shetter, R. E., Wert, B. P., and Fried, A.: Ozone production rates as a function of NO_x abundances and HO_x production rates in the Nashville urban plume, J. Geophys. Res., 107, D124146, doi:10.1029/2001JD000932, 2002.

Treves, K., Shragina, L., and Rudich, Y.: Henry's law constants of some β, γ, and δ hydroxy alkyl nitrates of atmospheric interest, Env. Sci. Tech., 34, 1197–1203, 2000.

Tuazon, E. C. and Atkinson, R.: A product study of the gas-phase reaction of methacrolein with the OH radical in the presence of NO_x, Int. J. Chem. Kinet., 22, 591–602, 1990.

von Kuhlmann, R., Lawrence, M. G., Crutzen, P. J., and Rasch, P. J.: A model for studies of tropospheric ozone and nonmethane hydrocarbons: Model description and ozone results, J. Geophys. Res., 108, 4294, doi:10.1029/2002JD002893, 2003.

von Kuhlmann, R., Lawrence, M. G., Pöschl, U., and Crutzen, P. J.: Sensitivities in global scale modeling of isoprene, Atmos. Chem. Phys., 4, 1–17, doi:10.5194/acp-4-1-2004, 2004.

Warneke, C., de Gouw, J. A., Del Negro, L., Brioude, J., McKeen, S., Stark, H., Kuster, W. C., Goldan, P. D., Trainer, M., Fehsenfeld, F. C., Wiedinmyer, C., Guenther, A. B., Hansel, A., Wisthaler, A., Atlas, E., Holloway, J. S., Ryerson, T. B., Peischl, J., Huey, L. G., and Case Hanks, A. T.: Biogenic emission measurement and inventories determination of biogenic emissions in the eastern United States and Texas and comparison with biogenic emission inventories, J. Geophys. Res., 115, D00F18, doi:10.1029/2009JD012445, 2010.

Weaver, C. P., Cooter, E., Gilliam, R., Gilliland, A., Grambsch, A., Grano, D., Hemming, B., Hunt, S. W., Nolte, C., Winner, D. A., Liang, X.-Z., Zhu, J., Caughey, M., Kunkel, K., Lin, J.-T., Tao, Z., Williams, A., Wuebbles, D. J., Adams, P. J., Dawson, J. P., Amar, P., He, S., Avise, J., Chen, J., Cohen, R. C., Goldstein, A. H., Harley, R. A., Steiner, A. L., Tonse, S., Guenther, A., Lamarque, J.-F., Wiedinmyer, C., Gustafson, W. I., Leung, L. R., Hogrefe, C., Huang, H.-C., Jacob, D. J., Mickley, L. J., Wu, S., Kinney, P. L., Lamb, B., Larkin, N. K., McKenzie, D., Liao, K.-J., Manomaiphiboon, K., Russell, A. G., Tagaris, E., Lynn, B. H., Mass, C., Salathé, E., O'neill, S. M., Pandis, S. N., Racherla, P. N., Rosenzweig, C., and Woo, J.-H.: A preliminary synthesis of modeled climate change impacts on U.S. regional ozone concentrations, B. Am. Meteorol. Soc., 90, 1843–1863, doi:10.1175/2009BAMS2568.1, 2009.

Whalley, L. K., Edwards, P. M., Furneaux, K. L., Goddard, A., Ingham, T., Evans, M. J., Stone, D., Hopkins, J. R., Jones, C. E., Karunaharan, A., Lee, J. D., Lewis, A. C., Monks, P. S., Moller, S. J., and Heard, D. E.: Quantifying the magnitude of a missing hydroxyl radical source in a tropical rainforest, Atmos. Chem. Phys., 11, 7223–7233, doi:10.5194/acp-11-7223-2011, 2011.

Wu, S., Mickley, L. J., Jacob, D. J., Logan, J. A., Yantosca, R. M., and Rind, D.: Why are there large differences between models in global budgets of tropospheric ozone?, J. Geophys. Res., 112, D05302, doi:10.1029/2006JD007801, 2007.

Zhu, T., Barnes, I., and Becker, K. H.: Relative-rate study of the gas-phase reaction of hydroxy radicals with difunctional organic nitrates at 298 K and atmospheric pressure, J. Atmos. Chem., 13, 301–311, doi:10.1007/BF00058137, 1991.